Electronic Supplementary Material (ESI) for Physical Chemistry Chemical Physics.

Design of an Efficient Photocatalyst: Type Ⅱ Heterojunction for Enhanced Hydrogen Production Driven by Visible Light

Jin Feng, [†] Mengdi Cui, [†] Huining Liu, [†] Fengjie Zhou, [†] Siwei Bi, [*†] Dapeng Zhang [*†]

[†] School of Chemistry and Chemical Engineering, Qufu Normal University, Qufu 273165, China

*Corresponding author: Dapeng Zhang; Siwei Bi.

E-mail: zdp1014636837@hotmail.com; siweibi@126.com.

Table of Contents

Free Energy Calculation

The process of oxygen evolution reaction (OER) is as following:

$H_2O + \ ^* \rightarrow OH^* + H^+ + e^-$ (1)

$OH^* \rightarrow O^* + H^+ + e^-$ (2)

$O^* + H2O(l) \rightarrow HOO^* + H^+ + e^-$ (3)

$HOO^* \rightarrow \ ^* + O_2(g) + H^+ + e^-$ (4)

In computational hydrogen electrode (CHE) model[1], the free energy of a proton-electron pair at 0V *vs* RHE is defined to be to ½ of the H_2 free energy at 101,325 Pa, meaning that the Gibbs free energy change (∆G)is 0 for the reaction $H^+_{(aq)} + e^- \rightleftharpoons \frac{1}{2}H_{2(g)}$. Therefore, the ∆G for each elemental step is

$$\Delta G_1 = G_{HO^*} + {}^1\!/\!_2 G_{H_2} - G_{*} - G_{H_2O}$$

$$\Delta G_2 = G_{O^*} + {}^1\!/\!_2 G_{H_2} - G_{OH*}$$

$$\Delta G_3 = G_{HOO^*} + {}^1\!/\!_2 G_{H_2} - G_{O^*} - G_{H_2O}$$

$$\Delta G_4 = 4.92 - [\Delta G_1 + \Delta G_2 + \Delta G_3]$$

The Gibbs free energy is calculated using

$$G = E + ZPE - TS + eU$$

where E is the energy of optimized structure; *e* and *U* are the number of electrons transferred and the electrode potential applied; the zero point energies (ZPE) and enthalpic entropy correction (TS) were obtained as G(T) using Vaspkit.[2]

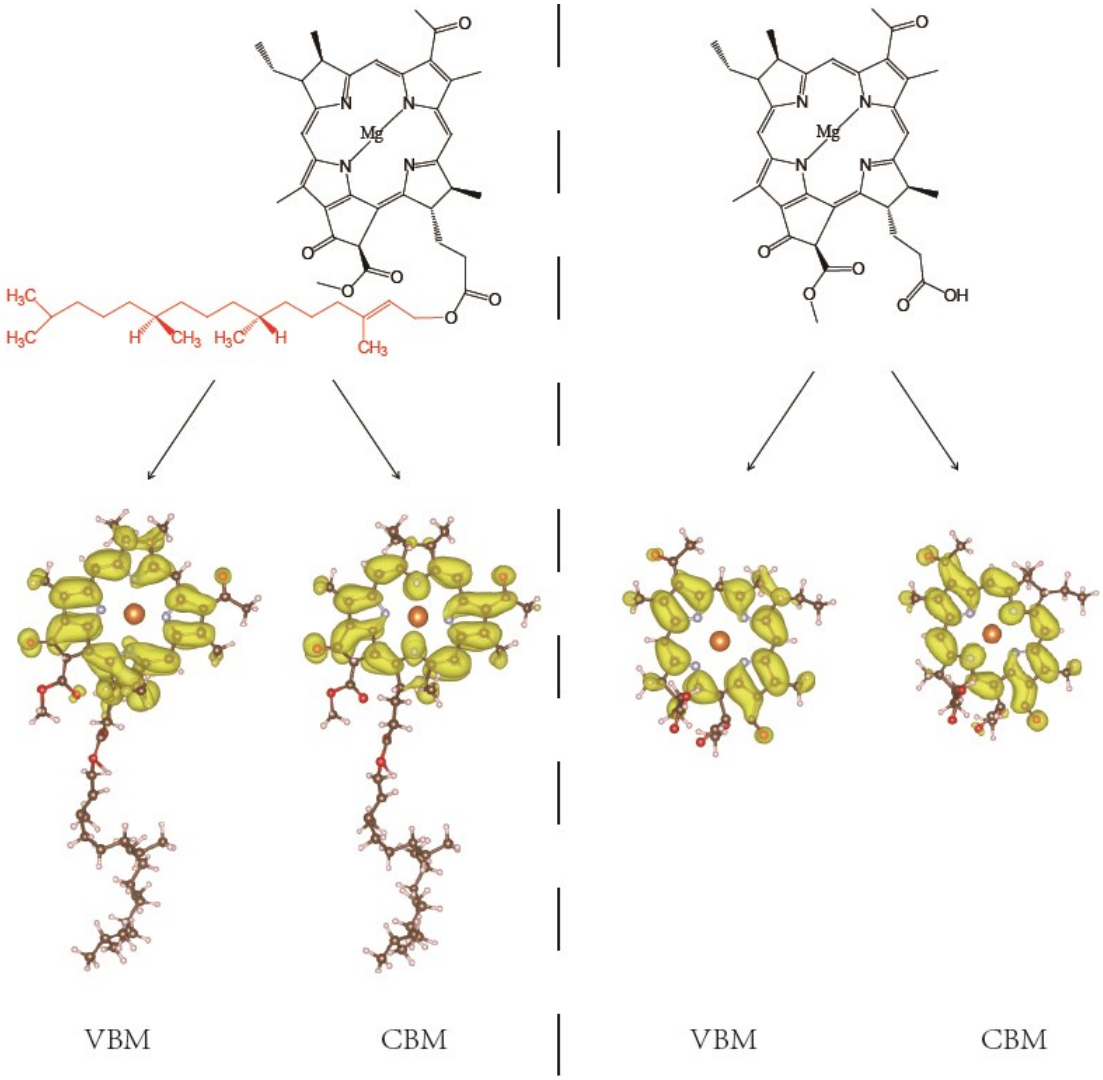

Figure S1. The structures and orbital distributions of chlorophyll (left) and simplified chlorophyll (right).

In our study, the reasons why phytyl chain longer than 10 Å shown in red in left of Figure S1 can be replaced by H are as follows: first, the frontier orbitals of Mg-chl which determines the type of heterojunction Mg-chl/g-C_3N_4 are fixed on the porphyrin structure, not the phytyl chain; second, the distance between the red phytyl chain and g-C_3N_4 is more than 12 Å resulting weak interaction between them.

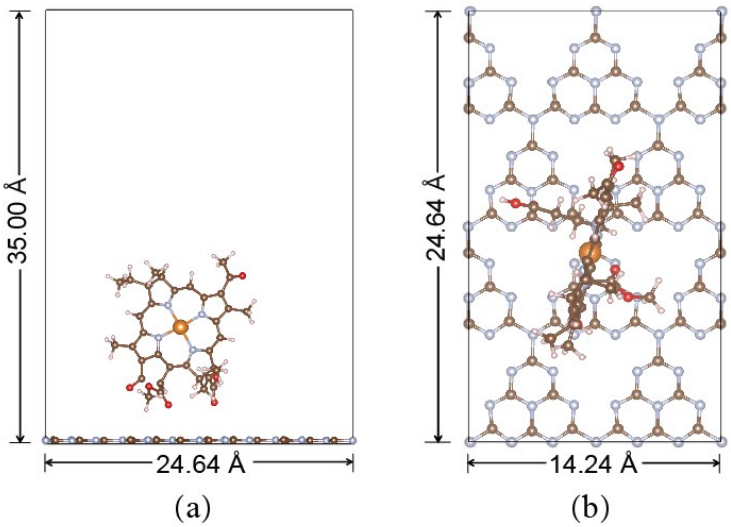

Figure S2 Side view (left) and top view (right) of Mg-chl/g-C_3N_4.

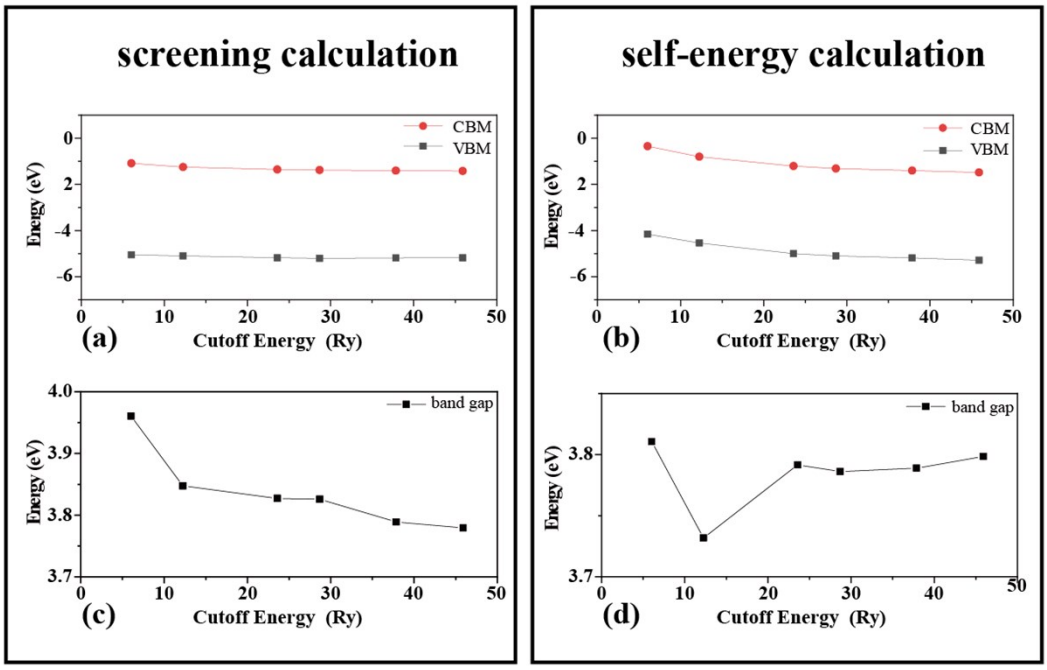

Figure S3 Calculated GW VBM and CBM energies of perfect g-C_3N_4 versus cutoff energy of unoccupied orbitals in the screening calculation(a) and self-energy calculation (c), while the band gaps shown in (c) and (d). The cutoff energy is relative to the CBM energy.

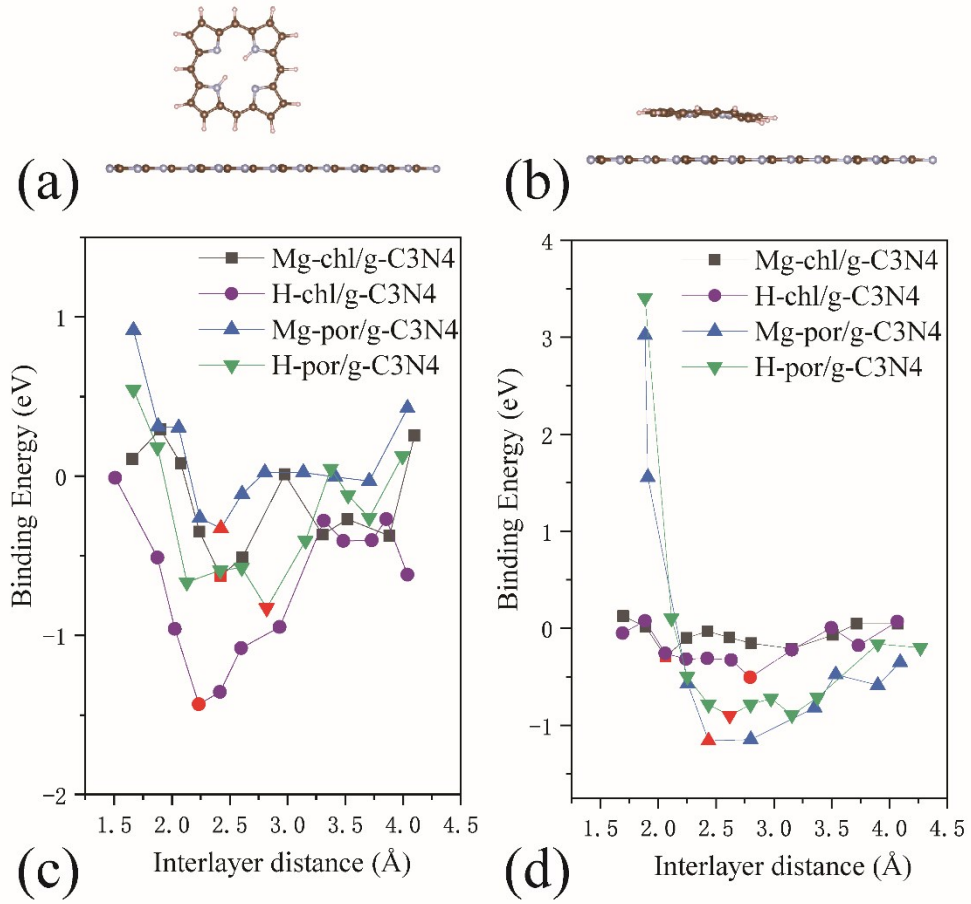

Figure S4. Two configurations of porphyrin relative to CN, vertical and parallel, are shown in (a) and (b). Binding energies of four porphyrins on the g-C_3N_4 monolayer for vertical (a) and parallel (b) configurations as a function of the distance between porphyrins and g-C_3N_4 are shown in (c) and (d). The optimal distance for each configuration is marked in red in (c) and (d).

The interlayer distance between porphyrin and g-C_3N_4 is the difference of between the maximum value of g-C_3N_4 in Z direction and the minimum value of porphyrin in Z direction. We set up several random stacking patterns by hand with interlayer distance ~3 Å when porphyrin is perpendicular or parallel to g-C_3N_4 (the configurations are shown in Figure S2(a) and S2(b)), then the interlayer distances from 1.5 to 4.3 Å of the most stable pattern are tested to find the stable configuration. We think that stacking pattern would influence little the electronic properties due to the long-range weak dispersion interaction between porphyrin and g-C_3N_4.

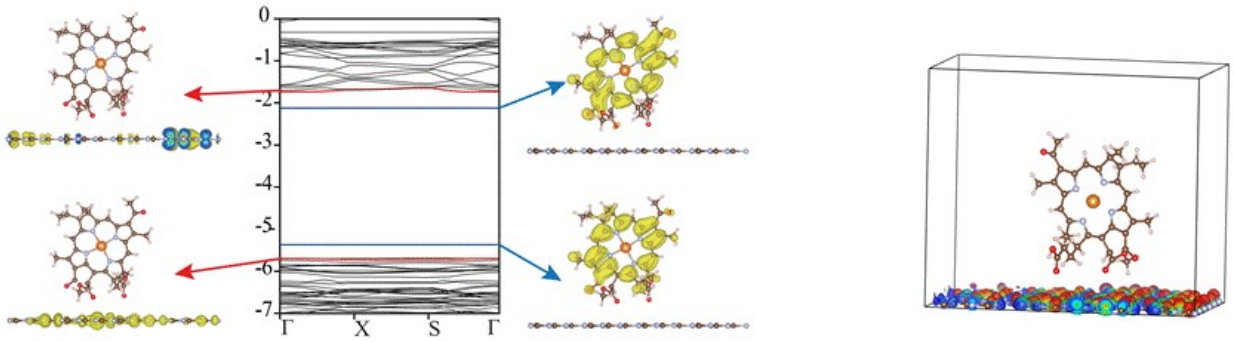

Figure S5 The left is band structure and orbital distribution of Mg-chl/g-C_3N_4, where the VBM and CBM of porphyrin (g-C_3N_4) are marked in blue (red). The right is the distribution of the electron (red) and hole (blue) for the first excited state.

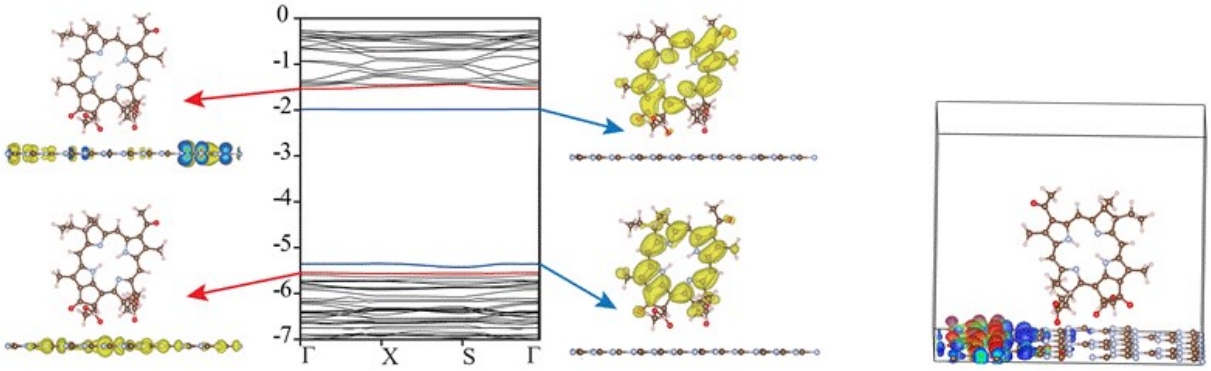

Figure S6 The band structure and orbital distribution of H-chl/g-C_3N_4, where the VBM and CBM of porphyrin (g-C_3N_4) are marked in blue (red).

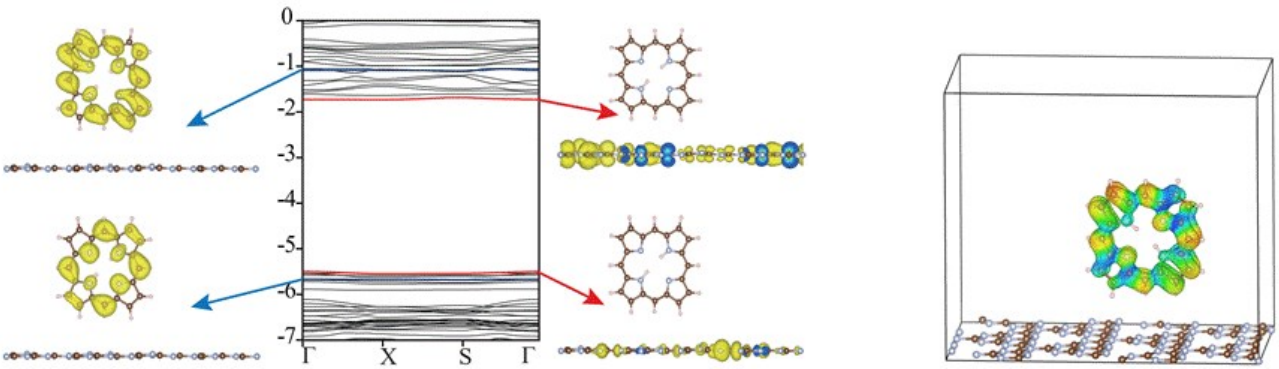

Figure S7 The left is band structure and orbital distribution of H-por/g-C_3N_4, where the VBM and CBM of porphyrin (g-C_3N_4) are marked in blue (red). The right is the distribution of the electron (red) and hole (blue) for the first excited state.

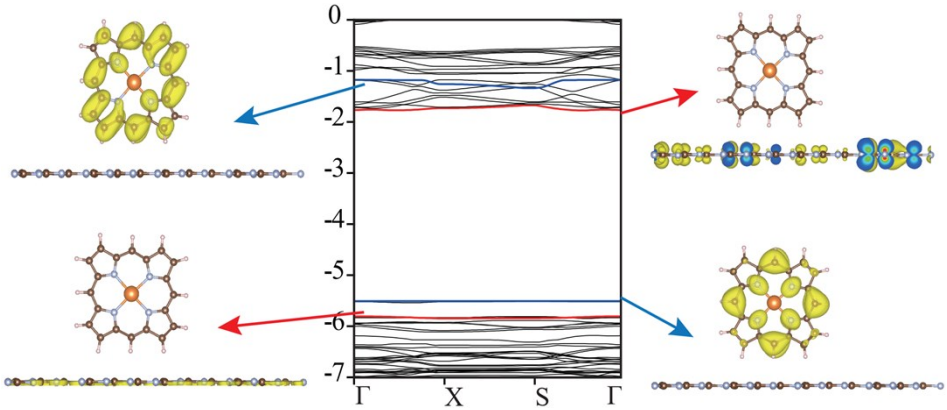

Figure S8 The band structure and orbital distribution of Mg-por/g-C_3N_4, where the VBM and CBM of porphyrin (g-C_3N_4) are marked in blue (red).

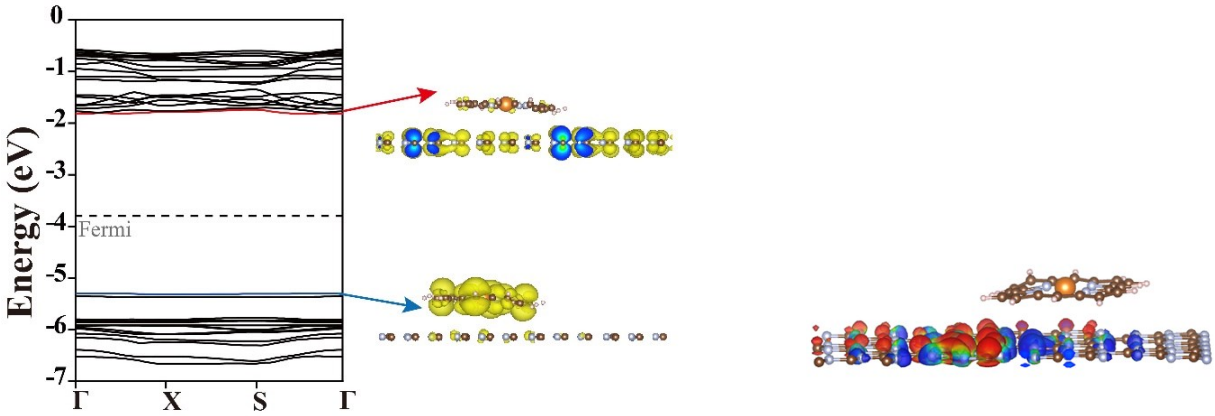

Figure S9 The left is band structure and orbital distribution of Mg-por/g-C_3N_4, where the VBM and CBM of porphyrin (g-C_3N_4) are marked in blue (red). The vacuum energies (Ev) of all materials are set to 0. The fermi level is marked with black dotted line. The right is the distribution of the electron (red) and hole (blue) for the first excited state.

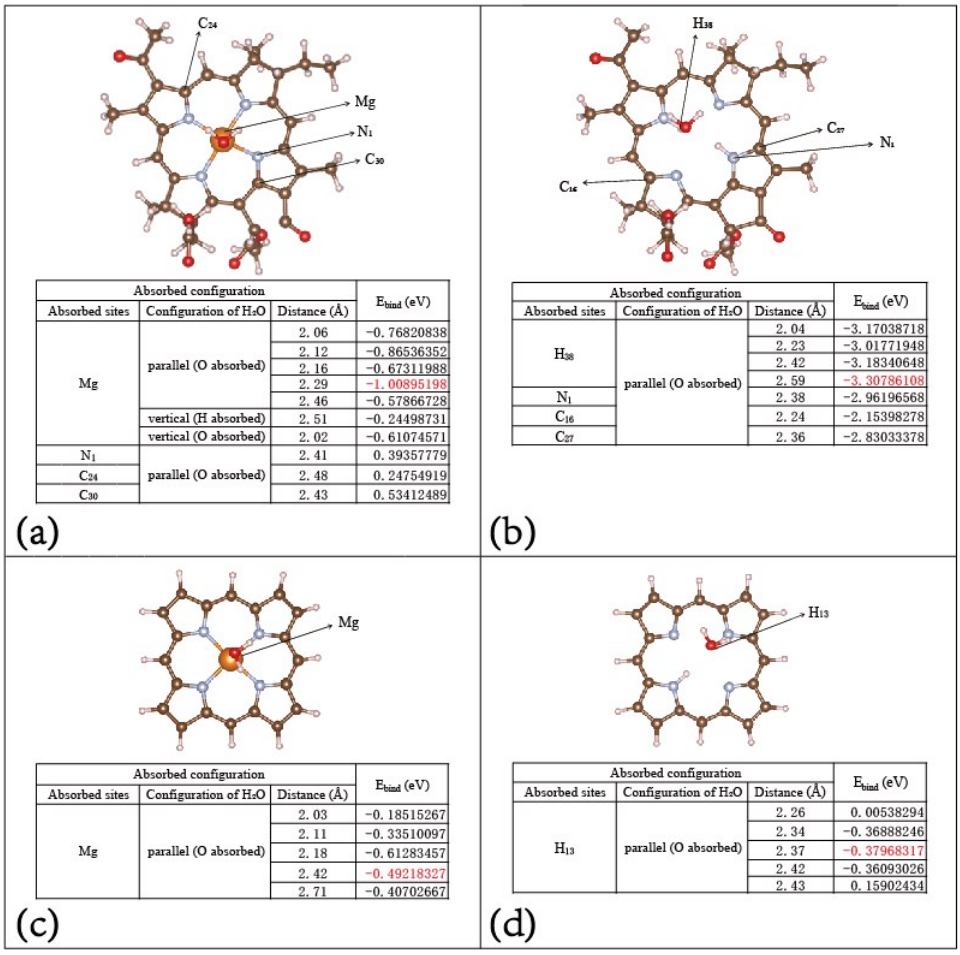

(a)

Absorbed configuration			E_{bind} (eV)
Absorbed sites	Configuration of H_2O	Distance (Å)	
Mg	parallel (O absorbed)	2.06	−0.76820838
		2.12	−0.86536352
		2.16	−0.67311988
		2.29	−1.00895198
		2.46	−0.57866728
	vertical (H absorbed)	2.51	−0.24498731
	vertical (O absorbed)	2.02	−0.61074571
N_1	parallel (O absorbed)	2.41	0.39357779
C_{24}		2.48	0.24754919
C_{30}		2.43	0.53412489

(b)

Absorbed configuration			E_{bind} (eV)
Absorbed sites	Configuration of H_2O	Distance (Å)	
H_{38}	parallel (O absorbed)	2.04	−3.17038718
		2.23	−3.01771948
		2.42	−3.18340648
		2.59	−3.30786108
N_1		2.38	−2.96196568
C_{16}		2.24	−2.15398278
C_{27}		2.36	−2.83033378

(c)

Absorbed configuration			E_{bind} (eV)
Absorbed sites	Configuration of H_2O	Distance (Å)	
Mg	parallel (O absorbed)	2.03	−0.18515267
		2.11	−0.33510097
		2.18	−0.61283457
		2.42	−0.49218327
		2.71	−0.40702667

(d)

Absorbed configuration			E_{bind} (eV)
Absorbed sites	Configuration of H_2O	Distance (Å)	
H_{13}	parallel (O absorbed)	2.26	0.00538294
		2.34	−0.36888246
		2.37	−0.37968317
		2.42	−0.36093026
		2.43	0.15902434

Figure S10 The configurations and binding energies for H_2O absorbing on Mg-chl (a), H-chl (b), Mg-por (c) and H-por (d). The absorbed sites include Mg, N and H atoms. The initial configurations of H_2O are divided into three types: the first is that H_2O is parallel to porphyrin with O atom absorbing on it; the second is that H_2O is perpendicular to porphyrin with its H atom absorbing on it; the third is that H_2O is perpendicular to porphyrin with its H atom absorbing on it. The binding energy is the optimal energy difference between the individual H_2O plus porphyrin and the H_2O/porphyrin.

•H-•OH	H_2O	H_2O+Mg-chl^n	H_2O+H-chl^n	H_2O+Mg-H^n	H_2O+H-H^n	H_2O+g-C_3N_4
Ed(n=0)	5.49	4.08	5.26	4.62	5.11	4.98
S(n=0)	10^{-32}	10^{-9}	10^{-29}	10^{-18}	10^{-26}	10^{-24}
Ed(n=1$^+$)		4.45	5.63	5.12	5.62	5.45
S(n=1$^+$)		10^{-15}	10^{-35}	10^{-26}	10^{-35}	10^{-32}
Ed(n=1$^-$)		2.92	4.66	2.80	4.49	4.47
S(n=1$^-$)		10^{11}	10^{-18}	10^{13}	10^{-16}	10^{-15}

Table S1 The dissociation energies (eV) for the •H (E_d) and the relative rates of H-O bond dissociation (S). The rate of H^+ production in Table 1 is regarded as unit 1. The values of n, 0, 1^+ and 1^- represent the neutral, losing electron and obatining electron states of porphyrin and g-C_3N_4.

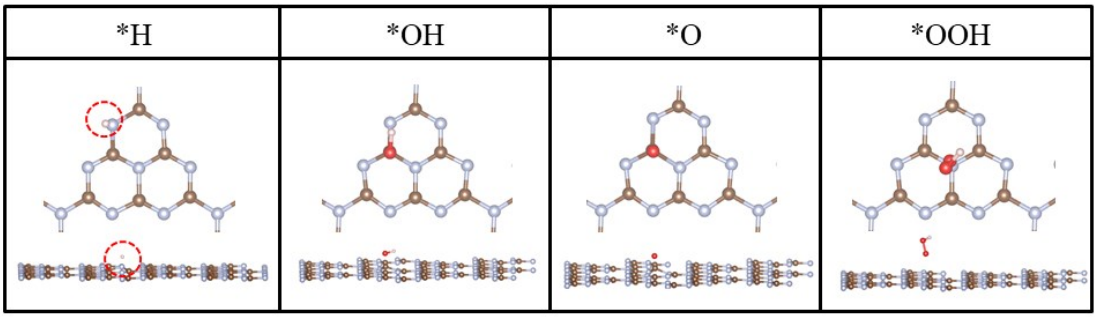

Figure S11 Structures of the reaction intermediates for H_2 (*H) and O_2 (*OH, *O and *OOH) on pure g-C_3N_4.

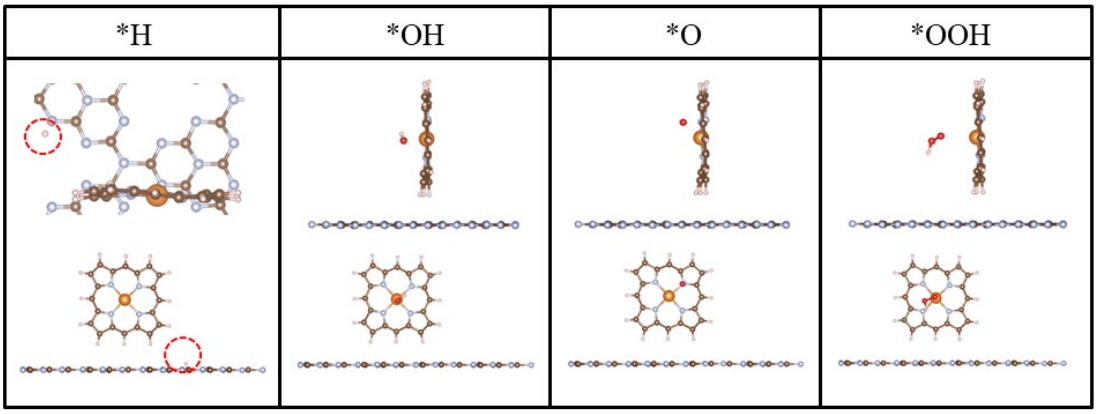

Figure S12 Structures of the reaction intermediates for H_2 (*H) and O_2 (*OH, *O and *OOH) on Mg-por/g-C_3N_4.

1. Jiao, Y.; Zheng, Y.; Chen, P.; Jaroniec, M.; Qiao, S. Z., Molecular Scaffolding Strategy with Synergistic Active Centers to Facilitate Electrocatalytic Co_2 Reduction to Hydrocarbon/Alcohol. *J. Am. Chem. Soc.* **2017**, *139*, 18093-18100.

2. Wang, V.; Xu, N.; Liu, J. C.; Tang, G.; Geng, W. T., Vaspkit: A Pre- and Post-Processing Program for Vasp Code. . *arXiv: Mater. Sci.* **2019**.